JOURNAL OF BACTERIOLOGY, Aug. 1980, p. 680-692
0021-9193/80/08-0680/13$02.00/0

Vol. 143, No. 2

Specificity in the Formation of Δ*tra* F-Prime Plasmids

R. G. HADLEY† AND RICHARD C. DEONIER*

Molecular Biology, Department of Biological Sciences, University of Southern California, Los Angeles, California 90007

Twenty-three independent Δ*tra* F-prime plasmids from three different *Escherichia coli* K-12 sublines were isolated from Hfr strains whose points of origin coincided with the IS*3* element $\alpha_3\beta_3$ or $\alpha_4\beta_4$ in the *lac-purE* region of the *E. coli* chromosome. Electrophoretic analysis of plasmid deoxyribonucleic acid digested with *Eco*RI and hybridization analysis of plasmid deoxyribonucleic acid digested with *Bgl*II revealed that at least 14 of these plasmids were formed by processes involving specific bacterial and F loci. Two of the specific bacterial loci involved in Δ*tra* F-prime formation were located at approximately 3.3 and 11.7 min on the *E. coli* chromosomal map. Two of the Δ*tra* F-prime plasmids contained bacterial deoxyribonucleic acid with circularization endpoints that mapped very near the termini of the IS*2* element that is normally located between *lac* and *proC*.

Hfr strains produce recombinants at a high frequency in matings with *recA*$^+$ F$^-$ bacteria of the same species. In addition, Hfr strains are known to produce different structural classes of autonomously replicating conjugative F-prime plasmids (22, 26, 28, 30). The Δ*tra* F-prime plasmids represent a class of nonconjugative F-prime plasmids that are formed after matings between an Hfr strain and a *recA* recipient with selection for proximal Hfr markers (17, 25). Since recombination is drastically reduced in *recA* strains (8), selected clones contain plasmid molecules that are capable of stable replication, but that lack the *tra* operon of F, which is the most distal region transferred in Hfr × F$^-$ matings. The Δ*tra* F-prime plasmids are therefore conjugationally defective.

Guyer et al. (17) determined the structure of certain members of this F-prime class by heteroduplex analysis of four independent Δ*tra* F*argG*$^+$ plasmids. Their study revealed that the only F sequences present on each plasmid were those extending from near the F-plasmid transfer origin (*oriT*) to the site at which the F plasmid had integrated into the bacterial chromosome. This verified that the transfer deficiency resulted from the complete absence of all transfer genes. Each of the Δ*tra* F*argG*$^+$ plasmids carried a different length of chromosomal DNA (126.9, 134.8, 152.6, and 243.3 kilobases [kb]), and the site on F at which circularization occurred varied in at least three of these four plasmids (62.0, 62.2, 52.2, and 58.5F).

In the present study, 23 independent Δ*tra* F-prime plasmids were analyzed by gel electrophoresis of *Eco*RI restriction endonuclease fragments, and 11 of these were further characterized by *Bgl*II digestion and by hybridization. Six of the plasmids were isolated from independent Hfr strains that had been formed by integration at the chromosomal IS*3* element $\alpha_3\beta_3$. The remaining 17 Δ*tra* F-prime plasmids were isolated from Hfr P3, which had been formed by integration at the chromosomal IS*3* element $\alpha_4\beta_4$ (28; R. G. Hadley, unpublished data). In contrast to the four Δ*tra* F*argG*$^+$ plasmids previously examined (17), over half of these new F-prime plasmids were formed by site-specific processes. The lengths of bacterial DNA carried by these plasmids define at least two regions on the *E. coli* chromosome at which site-specific circularization occurs.

MATERIALS AND METHODS

Bacterial strains. All bacteria used were derivatives of *E. coli* K-12 (Table 1). Genetic symbols within parentheses indicate genes that are expected to be present based on the length of the plasmid DNA but were not directly tested.

F-prime isolation. All Hfr strains used in F-prime isolation experiments were obtained from independent single-colony isolates, and the approximate points of origin and transfer gradients were verified by cross-streak matings with the *recA*$^+$ recipient strain AB1157 before F-prime isolation. The Δ*tra* F-prime plasmids were derived from these Hfr isolates after mating with the Str^r *recA* recipient AB2463 or ED1111 and selecting for *proA*$^+$ Str^r or *purE*$^+$ Str^r transconjugants, respectively. Matings were performed in L broth (24) and were interrupted by 1 min of violent agitation followed by chilling on ice, or by incubating with 2.5 × 10^{10} plaque-forming units of T6 per ml for 20 min at 37°C before chilling on ice. Matings were usually for 30 min. Interruptions after 4 to 8 min did not alter the classes of F-prime plasmids obtained. Isolates were purified on selective media (9) and were screened for transfer deficiency, sensitivity to UV light (a property

† Present address: Boyce Thompson Institute of Plant Research, Cornell University, Ithaca, NY 14853.

TABLE 1. *Bacterial strains*

Strain	Relevant genotype	Source and reference
F⁻		
AB1157	*thr-1 leu-6 thi-1 argE3 his-4 proA2 lacY1 galK2 ara-14 mtl-1 xyl-5 str-31 tsx-33*, λ⁻, *sup-37*	B. Bachmann (16)
AB2463	*thr-1 leu-6 thi-1 argE3 his-4 proA2 recA13 lacY1 galK2 ara-14 mtl-1 xyl-5 str-31 tsx-33 sup-37*	M. Guyer (20)
ED1111	*lac purE thi str recA*	N. Davidson (6)
JC10,173	JC3272(pRS27)	R. Skurray (32)
PB314	*lac purE tsx thi str*	N. Davidson (6)
RH65	PB314 Spc^r	This research
Hfr		
χ435(OR6)	Prototroph; derived from K-12-112	R. Curtiss (3, 13)
χ493(OR11)	Prototroph; derived from W1485	R. Curtiss (3, 13)
χ886(OR66)	Prototroph; derived from K-12-112	R. Curtiss (3, 13)
χ892(OR72)	Prototroph; derived from K-12-112	R. Curtiss (3, 13)
ED942(B5)	*metB1 rel-1*; derived from W1655	P. Broda (5)
ED943(B6)	*metB1 rel-1*; derived from W1655	P. Broda (5)
P3	*metB1 rel-1*; derived from W6	B. Bachmann (29)
Δ*tra*F*proA*⁺		
RH111	AB2463(pRH111); derived from Hfr OR6	This research
RH112	AB2463(pRH112); derived from Hfr OR11	This research
RH113	AB2463(pRH113); derived from Hfr OR66	This research
RH114	AB2463(pRH114); derived from Hfr OR72	This research
RH115	AB2463(pRH115); derived from Hfr B5	This research
RH116	AB2463(pRH116); derived from Hfr B6	This research
Δ*tra* F*purE*⁺, derived from P3		
RH100	ED1111(pRH100)	This research
RH101	ED1111(pRH101)	This research
RH126	ED1111(pRH126)	This research
RH127	ED1111(pRH127)	This research
RH129	ED1111(pRH129)	This research
RH133	ED1111(pRH133)	This research
RH135	ED1111(pRH135)	This research
RH99	ED1111(pRH99)	This research
RH128	ED1111(pRH128)	This research
RH134	ED1111(pRH132)	This research
Δ*tra* F*purE*⁺(*proC*⁺),[a] derived from P3		
RH130	ED1111(pRH130)	This research
RH131	ED1111(pRH131)	This research
RH132	ED1111(pRH132)	This research
Δ*tra* F*lac*⁺*purE*⁺(*proA*⁺), derived from P3		
RH139	ED1111(pRH139)	This research
RH140	ED1111(pRH140)	This research
RH141	ED1111(pRH141)	This research
RH142	ED1111(pRH142)	This research

[a] Genetic symbols within parentheses indicate genes that are expected to be present based on the length of the plasmid DNA but that were not directly tested.

of *recA* strains), and the absence of distal markers. F-prime isolates were stored at −20°C in 40% glycerol and 50% L broth immediately after marker analysis.

Plasmid DNA isolation. Plasmid DNA was isolated from *recA* transconjugant strains grown in minimal media with selection for genes carried by the F-prime as described (18). Approximately 0.035 μg of plasmid DNA was obtained per ml of culture medium.

Electrophoretic analysis and hybridization techniques. Restriction endonuclease digestion, agarose electrophoresis, mobility analysis, labeling, hybridization, and autoradiography were conducted as described previously (18). The average fragment sizes are stated to three significant figures, as determined by accuracies of the reference fragment sizes.

Restriction mapping conventions. To clarify subsequent analysis, the conventions used in the *Eco*RI mapping of the Δ*tra* F-prime plasmids are

summarized here. As seen in Fig. 1, these plasmids are expected to contain a length of F DNA which extends from near the F-plasmid transfer origin *oriT* counterclockwise along the F map to the site on F at which recombination occurred during Hfr formation. The length of bacterial sequences carried may vary for different plasmids. The restriction enzyme fragment containing the hybrid linkage of bacterial DNA to the F region near *oriT* will be referred to as the joint fragment. The altered restriction fragments containing the $\alpha\beta$ elements involved in integration are designated junction fragments. Each Δ*tra* F-prime plasmid will contain one joint fragment and one junction fragment.

Since exonucleolytic degradation may occur before plasmid circularization, it is not possible to determine the precise length of bacterial or F DNA present on the joint fragment from the map coordinates of *oriT*. Since *oriT* is located within the F-plasmid *Eco*RI fragment f6 (see, for example, reference 32) and in a 1.1-kb *Bgl*II fragment (33), Δ*tra* F-prime plasmids are expected to lack these fragments. Previous heteroduplex mapping analysis of four Δ*tra* F*argG*$^+$ plasmids indicated that differing lengths of F sequences are present in the region expected to be in the joint fragment, and that the average expected F endpoint within f6 is 62.1F, which is very near *oriT* (17). This allows the calculation that for Δ*tra* F-prime plasmids whose circularization event involves f6, approximately 2.2 kb of f6 is present on the joint fragment. Results to be presented in connection with the hybridization study indicate that part of the 1.1-kb *Bgl*II fragment b14 of F is present on the joint fragments produced from the three major classes of Δ*tra* F-prime plasmids. This confirms that at least 1.7 kb of fragment f6 is present in these plasmids (see Fig. 7).

RESULTS

Preliminary genetic analysis. Matings with Hfr donors in which F was integrated at $\alpha_3\beta_3$ (OR6, OR11, OR66, OR72, B5, or B6; see Table 1) yielded Δ*tra* F*proA*$^+$ plasmids as the major class, regardless of the mode of interruption. With selection for transmission of *proA*$^+$ to AB2463, Pro$^+$ transconjugants were obtained at frequencies of approximately 10^{-6} per input Hfr donor. The major category of transconjugants (70 to 100% of Pro$^+$ clones tested) carried *proA* but neither *leu* nor *lac*. The remaining Pro$^+$ clones showed joint inheritance of *lac* and *proA* or of *leu* (and sometimes *thr*) and *proA*. These strains, which apparently contain large F-prime plasmids, were not further characterized.

Matings between Hfr P3 (integrated at $\alpha_4\beta_4$) and ED1111, with selection for transmission of *purE*$^+$, yielded transconjugants at frequencies ranging from 2×10^{-7} to 2×10^{-6} for different experiments. Fifteen to twenty percent of the Pur$^+$ clones were Lac$^-$, and more than 95% of the Pur$^+$ Lac$^-$ clones were Tra$^-$, as judged by their inability to transfer *purE* to RH65. More than 80% of the Pur$^+$ transconjugants were Pur$^+$ Lac$^+$, and 50 to 80% of these were Tra$^+$, whereas the remainder were Tra$^-$. Thus, the major F-prime class obtained from Hfr P3 probably corresponds to the F *lac*$^+$ *proC*$^+$ *purE*$^+$ class, whose frequent appearance has been previously documented (3, 18).

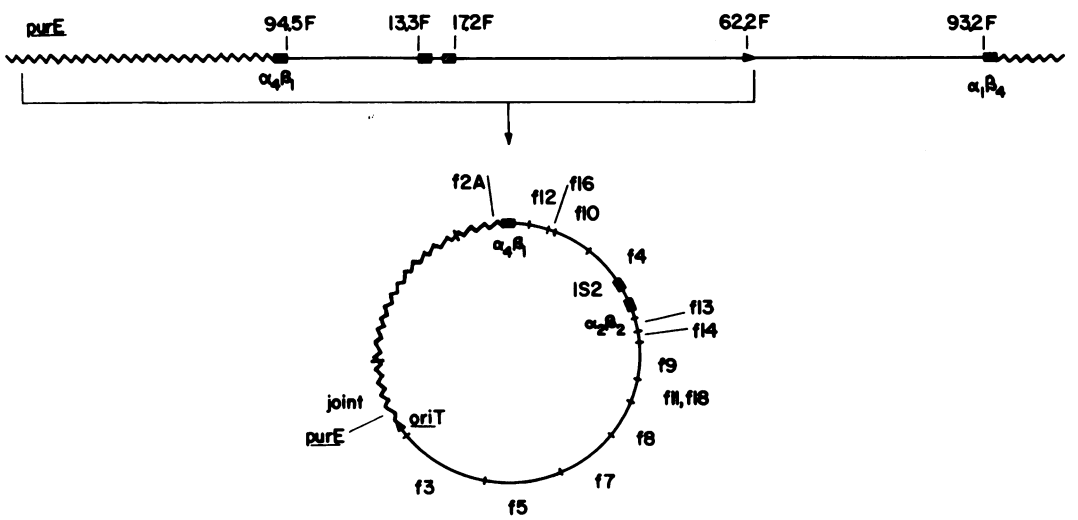

FIG. 1. *Schematic representation of the Hfr strain P3 and a Δtra FpurE*$^+$ *plasmid derived from P3. The integrated F sequences and the surrounding bacterial sequences are indicated at the top of the figure. Bacterial DNA is represented by sawtooth lines, and F sequences are identified by solid lines. A specific Δtra FpurE*$^+$ *plasmid that is derived from this region of the chromosome is represented as a circular structure. The F plasmid EcoRI fragments expected to be present on this type of Δtra F-prime are indicated.*

Δtra F*proA*$^+$ plasmids isolated from Hfr strains with F integrated at $\alpha_3\beta_3$. The Δtra F*proA*$^+$ plasmids pRH111, pRH112, pRH113, pRH114, pRH115, and pRH116 (Fig. 2) were derived from the independent Hfr strains OR6, OR11, OR66, OR72, B5, and B6, respectively. Each Hfr had formed by integration of F at the chromosomal $\alpha_3\beta_3$ sequence (14, 18). These Hfr strains were mated with the *recA proA* recipient AB2463, and Pro$^+$ Str^r transconjugants were selected. The resulting transconjugants were purified on selective media and were found to be unable to transfer *proA*$^+$, to be sensitive to UV, and to be Lac$^-$. F-prime DNA isolated from these transconjugant clones was digested with the *Eco*RI restriction endonuclease and subjected to agarose gel electrophoresis (Fig. 3) and mobility analysis. Each of the plasmids produced an *Eco*RI fragment distribution which was entirely consistent with their being Δtra F*proA*$^+$ plasmids. They contained fragments corresponding in size to the *Eco*RI fragments of F extending from the junction fragment clockwise to include the F plasmid *Eco*RI fragment f3, which was the *Eco*RI fragment immediately counterclockwise to f6 (see Fig. 1); they contained fragments corresponding in size to fragments from the *proA* region (i.e., those found in the F*lac*$^+$ *proA*$^+$ plasmid F128 but not in the F*lac* plasmid F42-1), and they each contained a fragment having the characteristic size of the junction fragment at $\alpha_3\beta_3$.

Four of these plasmids (pRH113 through pRH116) were found to generate almost identical fragment distributions (Fig. 3). The average sizes of the *Eco*RI fragments containing bacterial DNA for each are shown in Table 2. *Eco*RI fragments of F DNA have been omitted for simplification, and the average values represent data from 3- and 7-h electrophoretic experiments. The pRH114, pRH115, and pRH116 bacterial *Eco*RI fragments in the range of 4.4 to 4.7 kb were not clearly resolved because they comigrated with the *Eco*RI fragments f8, f9, and f10 of F. However, the intensity of this multiplet is consistent with the presence of either two or

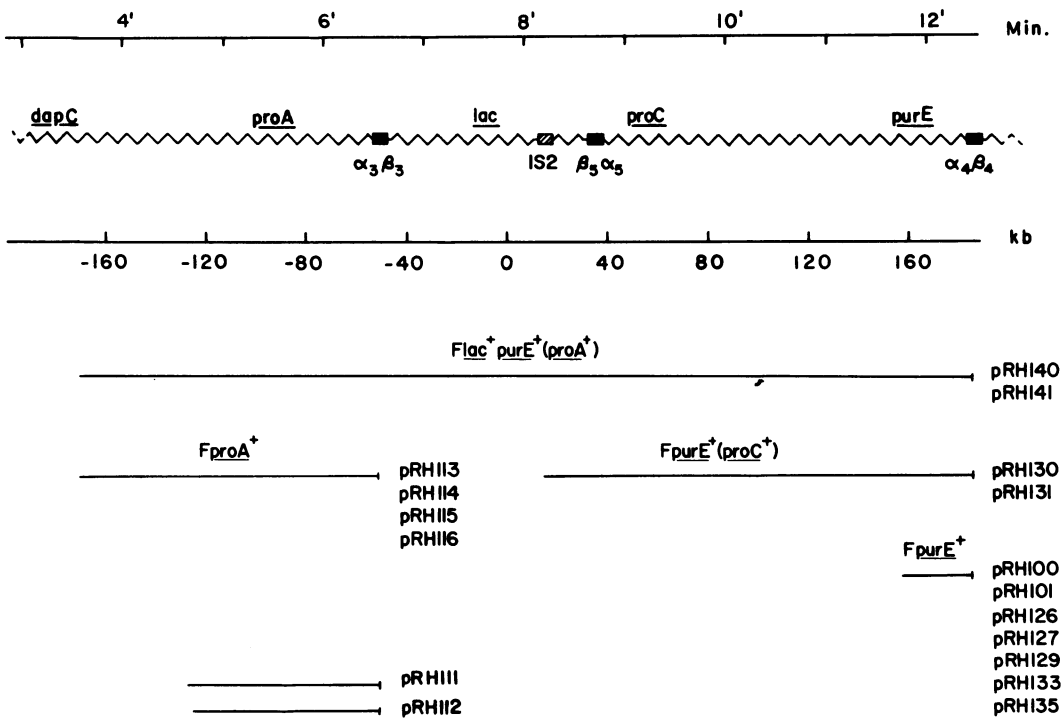

FIG. 2. *proA-purE region of the E. coli chromosome and lengths of bacterial DNA contained on different Δtra F-prime plasmids. The bacterial sequences are represented by a sawtooth line. The origin for the kilobase scale line is the EcoRI cleavage site in lacZ. Span lines indicate the lengths of bacterial DNA found on the plasmids indicated. Plasmids pRH111 and pRH112 did not contain bacterial DNA segments whose lengths indicated termination site specificity. All other plasmids shown were formed by site specific processes. The Δtra FproA*$^+$ *plasmids were formed from Hfr strains in which F was integrated at* $\alpha_3\beta_3$. *All other plasmids were formed from Hfr P3 (F integrated at* $\alpha_4\beta_4$*). The clockwise termini of the span lines are precisely mapped; the counterclockwise termini may vary by as much as 2.2 kb.*

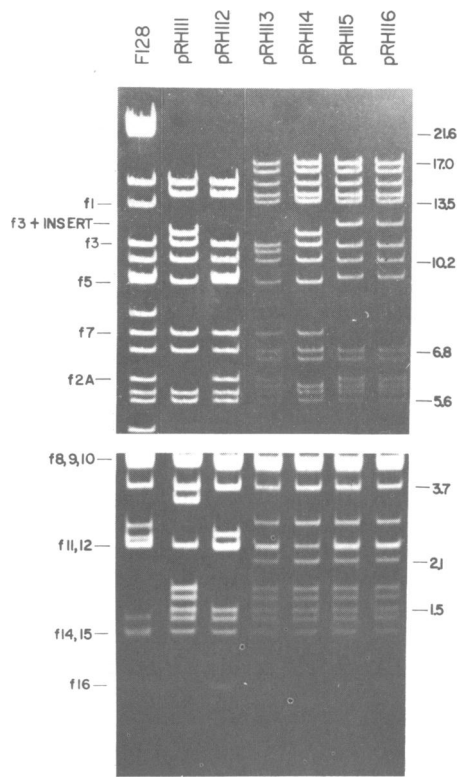

FIG. 3. *Electrophoretic analysis of EcoRI digests of several Δtra FproA⁺ plasmids and F128. pRH111 through pRH116 are Δtra FproA⁺ plasmids containing bacterial DNA immediately counterclockwise to $\alpha_3\beta_3$ (see Fig. 2). F128 contains bacterial DNA from both sides of $\alpha_3\beta_3$. The average sizes of the EcoRI fragments containing bacterial DNA from pRH113 through pRH116 are listed in Table 2. To represent fragments over an extended size range, the upper panel has been taken from a 7-h electrophoretic experiment, and the lower panel is from a different 3-h run. Selected EcoRI fragments of F are labeled, and the kilobase sizes of specific bacterial fragments are indicated. Fragment f3 in Hfr strains B5 and B6 contains an insertion leading to the modified f3 fragment (12.0 kb) seen for pRH115 and pRH116. The band near the normal f3 position in pRH115 and pRH116 is the f5-f8 fusion product resulting from the Δ(33–43) deletion. The junction fragments for pRH111 and pRH114 (11.4 kb) differ from the junction fragments of all the other Δtra FproA⁺ plasmids.*

three bacterial fragments, and F-prime plasmids derived from Hfr strains which had similar integration events had superimposable peaks in this region. The assignment of two bacterial fragments to this region is based on results from digestion with *Bgl*II discussed below.

The plasmids pRH113, pRH115, and pRH116 appeared to have identical distributions of fragments containing bacterial DNA, and these distributions differed from that of pRH114 by the presence of a 6.1-kb fragment and the absence of an 11.4-kb fragment. The progenitor Hfr strains of pRH113, pRH115, and pRH116 each contained F integrated at its $\alpha_1\beta_1$ sequence, whereas the progenitor Hfr of pRH114 contained F integrated at an IS*3* element located at 11.5F on the F map (18). This suggests that the 6.1-kb fragment may represent the junction of the F plasmid IS*3* element $\alpha_1\beta_1$ and the bacterial sequences counterclockwise of $\alpha_3\beta_3$ (f2A), whereas the 11.4-kb fragment represents the corresponding pRH114 junction fragment (f4A). This was confirmed by hybridization studies and heteroduplex analysis of other plasmids from the same Hfr strains (18). From the sizes of the junction fragments of pRH113, pRH115, and pRH116 (6.1 kb) and the amount of F DNA they contain, one can calculate that 3.3 kb of bacterial DNA is present, which agrees with the value of 3.3 kb calculated from the size of the 11.4-kb junction fragment of pRH114. Since the junction fragment of pRH114 differs in size from the junction fragments of pRH113, pRH115, and pRH116, it clearly represents an independent

TABLE 2. *Δtra FproA⁺ plasmid EcoRI fragments containing bacterial DNA sequences*

Fragment size[a]				
pRH113	pRH114	pRH115	pRH116	Avg
16.9	17.0	17.1	17.0	17.0
16.2	16.2	16.3	16.3	16.2
15.0	15.0	15.0	14.8	15.0
13.9	14.0	14.0	14.0	14.0
13.5	13.5	13.6	13.6	13.6
	11.4[b]			11.4
10.2	10.2	10.2	10.2	10.2
6.84	6.83	6.83	6.90	6.82
6.63	6.61	6.63	6.67	6.64
6.06[c]		6.08[c]	6.14[c]	6.09
5.93	5.97	5.98	5.97	5.96
5.78	5.82	5.84	5.81	5.81
5.57	5.63	5.59	5.65	5.61
4.58	+[d]	+	+	4.58
4.43	+	+	+	4.43
3.68	3.64	3.62	3.68	3.66
2.83	2.80	2.78	2.87	2.82
2.14	2.12	2.11	2.16	2.13
1.77	1.74	1.74	1.78	1.76
1.64	1.62	1.63	1.65	1.64
1.52	1.48	1.48	1.52	1.50
0.72	0.70	0.70	0.70	0.70
0.5	0.50	0.50	0.50	0.50

[a] Values represent average kilobase sizes determined by gel electrophoresis.
[b] pRH114 junction fragment (see text).
[c] f2A junction fragment.
[d] +, Size could not be determined accurately since these fragments comigrated with other F fragments. The multiple band was evaluated by densitometry.

isolate. In addition, pRH115 and pRH116 are derived from the W1655F$^+$ genetic background, and their F sequences are characteristically altered by the FΔ (33–43) deletion, which eliminates f5, f7, and f8 (Fig. 3), and by the presence of a 12.0-kb fragment resulting from an uncharacterized insertion in f3 (18).

As previously discussed, the amount of F DNA present on the joint fragment generated by *Eco*RI can be estimated to be approximately 2.2 kb. The total average size of the bacterial and joint fragments on pRH113 through pRH116 is 140 kb. By adding 3.3 kb of bacterial DNA carried on the junction fragment and subtracting the 2.2 kb of F DNA estimated to be carried on the joint fragment, one can estimate the length of bacterial DNA carried by these plasmids to be approximately 142 kb. A similar calculation based on electrophoretically resolved *Bgl*II fragments (data not shown) also indicates that the length of the bacterial segment in these plasmids is 142 kb. The other two Δ*tra* F*proA*$^+$ plasmids characterized, pRH111 and pRH112, contained approximately 80 and 76 kb of bacterial DNA, respectively.

Δ*tra* F*purE*$^+$ plasmids isolated from Hfr P3. Thirteen independent Δ*tra* F*purE*$^+$ plasmids were obtained after mating the Hfr strain P3 with the *recA* recipient ED1111 and selecting for Pur$^+$ Str^r transconjugants. These transconjugants were purified on selective media and were found to be unable to transfer *purE*$^+$, to be sensitive to UV, and to be Lac$^-$.

Seven of these F-prime plasmids were very similar, as can be seen from the distributions of *Eco*RI fragments that contain bacterial DNA shown in Table 3. Experiments for six of these plasmids are shown in Fig. 4. Each of these Δ*tra* F*purE*$^+$ plasmids had four *Eco*RI fragments that contained bacterial DNA sequences. These plasmids fell into one of two classes distinguished by the presence of either a 12.2- or 11.7-kb *Eco*RI fragment. These fragments are identified as the joint fragments since they are the only fragments not found in similar plasmids that contain a greater length of bacterial DNA (e.g., Table 4). The 7.2-kb fragment is the junction fragment, whereas the 14.9- and 9.5-kb fragments are bacterial fragments from the *purE* region (Fig. 4 and 5; 18).

Since Hfr P3 has been shown to have formed by recombination between the F-plasmid $\alpha_1\beta_1$ element and the chromosomal $\alpha_4\beta_4$ element (28; Hadley, unpublished data), the length of F DNA present in the 7.2-kb junction fragment can be calculated to be approximately 2.8 kb. As previously discussed, the joint fragment is expected to contain up to 2.2 kb of F DNA. The average length of *Eco*RI fragments composed wholly or partly of bacterial DNA in these plasmids is 43.6 kb (Table 3). This indicates that the total length of bacterial DNA carried by these plasmids is approximately 38.6 kb.

The bacterial sequences of the other six Δ*tra* F*purE*$^+$ (Fig. 5) did not terminate at the above-mentioned site. Three plasmids (pRH99, pRH128, and pRH134) were found to contain different lengths (122, 76, and 93 kb, respectively) of bacterial DNA, and three plasmids (pRH130, pRH131, and pRH132) were found to terminate at different positions within a single *Eco*RI fragment. The sizes of the *Eco*RI fragments that contained bacterial DNA of these three Δ*tra* F*purE*$^+$ (*proC*$^+$) plasmids are shown in Table 4. The bacterial and junction fragments found in the Δ*tra* F*purE*$^+$ plasmids shown in Table 3 were seen to be present, whereas the joint fragments of the Δ*tra* F*purE*$^+$ plasmids were clearly missing. This is expected since these Δ*tra* F*purE*$^+$ (*proC*$^+$) plasmids circularized at a bacterial site much further counterclockwise to *purE*. Although these three plasmids terminated within the same bacterial *Eco*RI fragment, the different sizes of the joint fragments (4.2, 5.7, and 15.9 kb) indicated that at least one of the sites involved in plasmid formation was variable. The amounts of bacterial DNA carried by pRH131 and pRH130 were approximately 178 and 177 kb, respectively, which agrees with the results obtained by using digestion with *Bgl*II

TABLE 3. *Δtra FpurE*$^+$ *plasmid EcoRI fragments containing bacterial DNA sequences*

Fragment size[a]							
pRH126	pRH127	pRH129	pRH135	pRH133	pRH100	pRH101[b]	Avg
14.8	14.8	14.8	15.2	14.8	14.9	15.1	14.9
				12.2	12.2	12.30	12.2
11.7	11.6	11.6	11.8				11.7
9.48	9.52	9.44	9.50	9.53	9.60	9.73	9.54
7.04	7.13	7.06	7.27	7.14	7.20	7.21	7.15

[a] Values represent average kilobase sizes as determined by gel electrophoresis.

[b] *Eco*RI fragment distribution of pRH101 produced densitometer traces that were superimposable with those of pRH100 (data not shown).

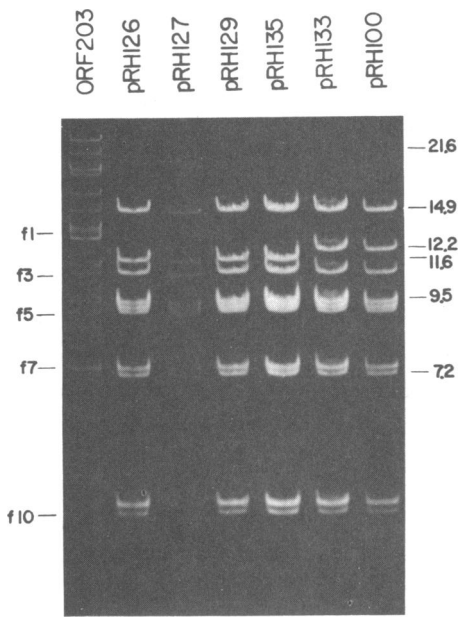

FIG. 4. *Electrophoretic analysis of EcoRI digests of several Δtra FpurE⁺ plasmids and ORF203. The Δtra F-prime plasmids contain bacterial DNA immediately counterclockwise to $\alpha_4\beta_4$ (see Fig. 2). ORF203 is an Flac⁺ proC⁺ purE⁺ plasmid that contains bacterial DNA from $\alpha_4\beta_4$ counterclockwise to $\alpha_3\beta_3$. The 14.9- and 9.5-kb fragments are from bacterial DNA in the purE region, and they are found in each of the plasmids shown. The average sizes of the EcoRI fragments containing bacterial DNA from these Δtra FpurE⁺ plasmids are shown in Table 3. Selected EcoRI fragments of F are labeled, and the kilobase sizes of specific bacterial fragments are indicated.*

(179 and 176 kb, respectively). Since $\alpha_4\beta_4$ is 239 kb from $\alpha_3\beta_3$ (18, 22), the bacterial endpoints involved in formation of pRH131 and pRH130 would map approximately 60.4 and 61.9 kb clockwise to $\alpha_3\beta_3$, respectively. The two termini of an IS*2* element have previously been mapped in this region by heteroduplex techniques at an average distance of 60.9 and 62.2 kb clockwise to $\alpha_3\beta_3$ (15, 22). The correspondence in these positions with the termination sites for pRH130 and pRH131 suggests the possibility of IS*2* involvement in the formation of these plasmids. Plasmid pRH132 contained bacterial DNA extending an additional 11.7 kb counterclockwise to the pRH130 termination site. None of the *Δtra* F-prime plasmids terminated near the bacterial IS*3* element $\alpha_3\beta_3$ or $\alpha_5\beta_5$.

Δtra Flac⁺ purE⁺ (proA⁺) plasmids isolated from Hfr P3. Four independent *Δtra* Flac⁺ purE⁺ plasmids were obtained by mating the Hfr P3 strain with the *recA* recipient ED1111 as described. At least two of these plasmids (pRH140 and pRH141) had bacterial termini that were identical within the resolution of these experiments. Electrophoretic analysis of *Eco*RI-digested DNA from these *Δtra* Flac⁺ purE⁺ (*proA*⁺) plasmids (Fig. 6) revealed 62 fragments larger than 0.8 kb for each plasmid, and indicated that each plasmid contained approximately 364 kb of bacterial DNA. The *Eco*RI fragment distribution of pRH142 ap-

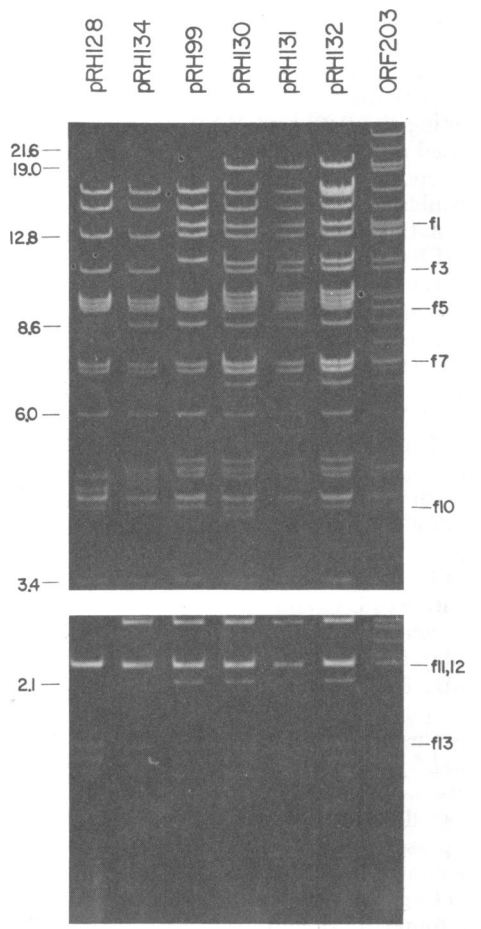

FIG. 5. *Electrophoretic analysis of EcoRI digests of pRH128, pRH134, pRH99, pRH130, pRH131, pRH132, and ORF203. The Δtra F-prime plasmids contain bacterial DNA extending from $\alpha_4\beta_4$ counterclockwise beyond the purE region. pRH130, pRH131, and pRH132 are Δtra FpurE⁺ (proC⁺) plasmids that formed by circularization within the same bacterial EcoRI fragment (Fig. 2, Table 4). pRH128, pRH134, and pRH99 (not shown in Fig. 2) each contain different lengths of bacterial DNA. Many of the fragments from these plasmids comigrate with fragments from ORF203. Data for 7- and 3-h experiments are combined as in Fig. 3. Selected EcoRI fragments of F are labeled, and the kilobase sizes of specific bacterial fragments are indicated.*

peared identical to that of pRH140 and pRH141 on the basis of one experiment (data not shown), but the DNA yields for this plasmid were insufficient for complete characterization.

Since the number, sizes, and regional distribution of the bacterial *Eco*RI fragments located between $\alpha_4\beta_4$ and $\alpha_3\beta_3$ are known (18), the bacterial *Eco*RI fragments counterclockwise to $\alpha_3\beta_3$ contained on these plasmids can be identified. Plasmids pRH140 and pRH141 contained fragments corresponding to all of the bacterial DNA between $\alpha_3\beta_3$ and $\alpha_4\beta_4$. Moreover, comparison of the pRH140 and pRH141 fragments with the *Eco*RI fragments contained in the Δ*tra* F*proA*$^+$ plasmids shown in Table 2 indicates that the bacterial endpoints of both classes of F-prime plasmids are identical. Except for the Δ*tra* F*proA*$^+$ junction fragments, each of the Δ*tra* F*proA*$^+$ *Eco*RI fragments that contained bacterial DNA was also present in the two Δ*tra* F*lac*$^+$ *purE*$^+$ (*proC*$^+$) plasmids. Moreover, the Δ*tra* F*lac*$^+$ *purE*$^+$ (*proA*$^+$) plasmids did not contain additional *Eco*RI fragments other than those expected from the $\alpha_3\beta_3$ region (Fig. 6). This suggests that a specific site on the bacterial DNA

TABLE 4. *Δtra FpurE*$^+$*(proC*$^+$*) plasmid EcoRI fragments containing bacterial DNA sequences*

Fragment size[a]			
pRH130	pRH131	pRH132	Avg
19.0	19.0	19.0	19.0
16.4	16.2	16.2 (15.9)[b]	16.3
14.8	14.8	14.7	14.0
13.5	13.4	13.6	13.5
12.8	12.8	12.8	12.8
11.3	11.2	11.3	11.0
9.75	9.84	9.81	9.80
9.53	9.58	9.54	9.55
8.57	8.60	8.57	8.58
7.28	7.30	7.29	7.29
7.11	7.13	7.11	7.12
7.11	7.13	7.11	7.12
6.75	6.75	6.73	6.74
6.03	6.04 (5.67)	6.00	6.02
5.09	5.11	5.06	5.09
4.97	4.97	4.93	4.96
4.84 (4.20)	4.85	4.81	4.83
3.38	3.42	3.36	3.39
3.13	3.14	3.11	3.13
2.13	2.15	2.10	2.13
1.17	1.18	1.14	1.16
1.17	1.18	1.14	1.16
1.03	1.05	1.02	1.03
0.91	0.93	0.88	0.91

[a] Values represent average kilobase sizes as determined by gel electrophoresis.

[b] Joint fragments are indicated by parentheses.

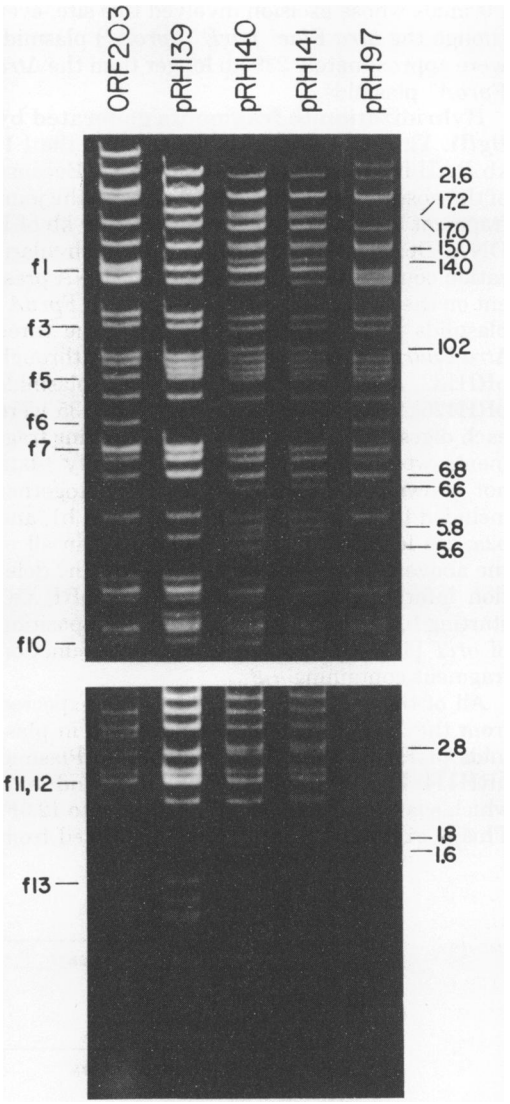

FIG. 6. *Electrophoretic analysis of EcoRI digests of pRH139, pRH140, and pRH141. Plasmids pRH139 through pRH141 contain bacterial DNA which extends from $\alpha_4\beta_4$ counterclockwise beyond $\alpha_3\beta_3$ (see Fig. 2). Bacterial DNA between $\alpha_3\beta_3$ and $\alpha_4\beta_4$ appears on both ORF203 and pRH97. pRH97 contains five additional fragments counterclockwise to $\alpha_3\beta_3$ that are not found on ORF203. Their sizes are 6.8 5.6, 4.5, 3.6, and 0.5 kb. Selected EcoRI fragments of F are labeled, and the kilobase sizes of specific bacterial fragments are indicated. Data for 7- and 3-h experiments are combined as in Fig. 3.*

counterclockwise to *proA* is involved in the formation of both types of Δ*tra* F-prime plasmids, regardless of the site of integration of F in the Hfr. There was no detectable variability in the bacterial DNA endpoints carried by F-prime

plasmids whose excision involved this site, even though the Δ*tra* F*lac*$^+$ *purE*$^+$ (*proA*$^+$) plasmids were approximately 239 kb longer than the Δ*tra* F*proA*$^+$ plasmids.

Hybridization to fragments generated by *Bgl*II. The *oriT* locus of F is located in the 1.1-kb *Bgl*II fragment b14 of F (33; Fig. 7). Because of the position of *oriT* on this fragment, the joint fragment could contain as much as 0.50 kb of F DNA. Degradation of F DNA during circularization could reduce the amount of F DNA present on the joint fragment. The four Δ*tra* F*proA*$^+$ plasmids pRH113 through pRH116, the three Δ*tra* F*purE*$^+$ (*proC*$^+$) plasmids pRH130 through pRH132, and the four Δ*tra* F*purE*$^+$ plasmids pRH126, pRH127, pRH129, and pRH135 were each digested with *Bgl*II, and the resulting fragments were resolved electrophoretically (data not shown). Three fragments which together included the entire *tra* region of F (b14, b1, and b2a; see legend to Fig. 7) were absent in all of the above cases, confirming the size of the deletion inferred from digestion with *Eco*RI, i.e., starting from the vicinity of 62.2F (the position of *oriT* [17]) and proceeding into the junction fragment containing $\alpha_1\beta_1$.

All of the other 12 *Bgl*II fragments expected from the F DNA were present, except in plasmids pRH114, pRH115, and pRH116. Plasmid pRH114 lacked fragments b6, b12, and b13, which spanned the region of F from 2.8 to 12.0F. This is expected since pRH114 is derived from an Hfr in which F is integrated at 11.5F (18). This places F sequences from 0.0 to 11.5F in the region that is transferred late in a mating; therefore, the portion of F from 0.0 to 11.5F is not recovered in this type of F-prime plasmid. The F sequences of plasmids pRH115 and pRH116 differed from the others by the absence of *Bgl*II fragments b4, b7, and b9, which lie in the region of the Δ(33–43) deletion of F sequences expected for plasmids derived from ΔF(33–43) and by the presence of an additional 3.5-kb hybrid fragment generated by the deletion. In addition to these changes arising from the Δ(33–43) deletion, b2b was missing in pRH115 and pRH116 (Fig. 8). As indicated in the discussion of the fragments produced from these plasmids by *Eco*RI, there was a 1.3-kb insertion in the region of F DNA spanned by b2b and f3 (see Fig. 7). This led in the case of digestion by *Eco*RI to an altered f3 with larger molecular size. In the case of digestion with *Bgl*II, two fragments (8.9 and 7.2 kb) characteristic of pRH115 and pRH116 and absent from pRH113 and pRH114 were found. The sum of the sizes of these fragments was 16.1 kb, approximately equal to the sum of the sizes of b2b and the insert. The conclusion is that the insertion in f3 and b2b is cleaved by *Bgl*II, a conclusion that is supported by the hybridization results described below.

DNA of the 11 plasmids indicated above and F-plasmid DNA was digested with *Bgl*II and resolved electrophoretically, transferred to ni-

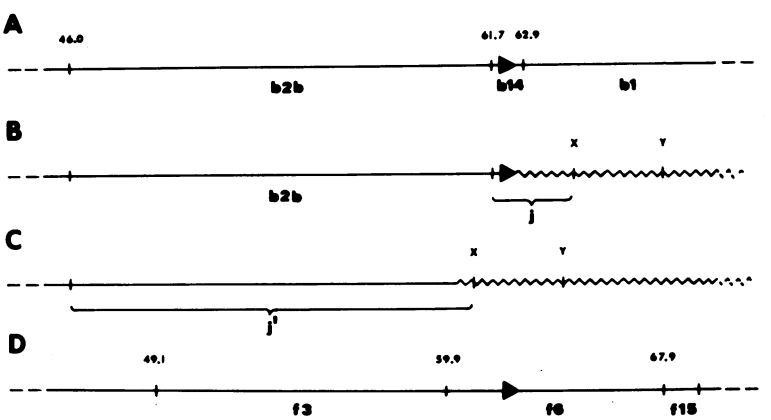

FIG. 7. *Cleavage sites for BglII in the vicinity of oriT on F and on hypothetical Δtra F-prime plasmids. (A) F DNA. Fragment b2a (not shown in the figure) is located immediately clockwise of b1, and it contains the distal portion of the tra region (R. G. Hadley and R. C. Deonier, unpublished data). Fragments b2a and b2b comigrate under our electrophoretic conditions. (B, C) Sequence organization of two possible Δtra F-prime plasmids, one of which is formed with little or no degradation of DNA at oriT (B) and the other of which has lost DNA from oriT up to a position counterclockwise to the BglII site at 61.7F, which defines the counterclockwise terminus of b14 (C). Arbitrary bacterial BglII sites are labeled X and Y. The two joint fragments (j and j') differ with respect to bacterial and F sequences that they contain. Joint j contains F DNA derived from b14, whereas j' contains F DNA derived from b2b. The plasmids described in this study have the arrangement shown in panel B rather than the one in panel C. (D) EcoRI cleavage sites in the region of F corresponding to panel A. Fragment f6 is seen to overlap b14 and the clockwise portion of b2b. Both of the joint fragments depicted in panels B and C will hybridize to fragment f6 DNA.*

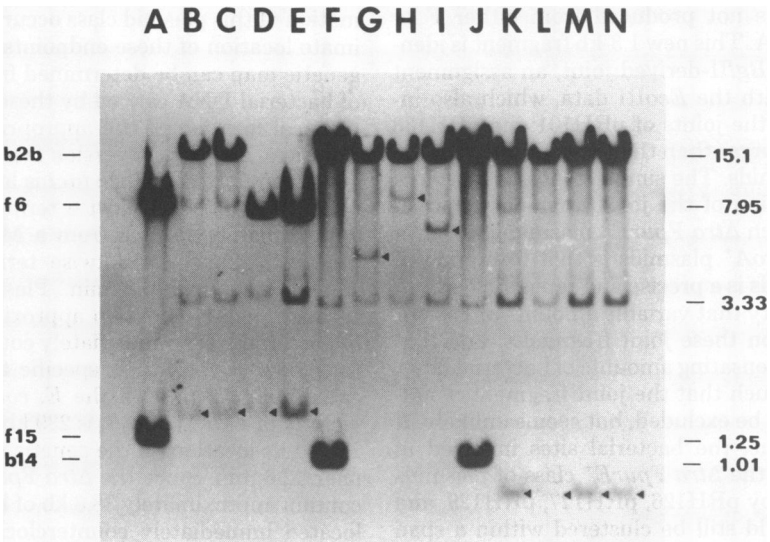

FIG. 8. *Hybridization of ^{3}H-labeled pRS27 DNA to electrophoretically resolved BglII digests of Δtra F-prime plasmids. (A) F-plasmid DNA digested with EcoRI; (F, J) F DNA digested with BglII. EcoRI or BglII fragments of F that hybridize with f6 or f15 derived from the pRS27 probe are indicated on the left, and fragment sizes in kilobases are displayed on the right. (B-E) DNA from the Δtra FproA$^+$ plasmids pRH113, pRH114, pRH115, and pRH116, respectively. (G-I) DNA from Δtra FpurE$^+$ (proC$^+$) plasmids pRH130, pRH132, and pRH131, respectively. (K-N) DNA from plasmids Δtra FpurE$^+$ pRH126, pRH127, pRH129, and pRH135. The joint fragments are identified by triangles.*

trocellulose filter paper, and hybridized to plasmid pRS27, which contains *Eco*RI fragments f6 and f15 of F joined to pSC101 (32). The hybridization patterns obtained are shown in Fig. 8. With the exception of pRH115 and pRH116, all plasmids, including the F control, showed faint hybridization bands that comigrated with *Bgl*II fragment b4 or b5 and with fragment b7 of F. These hybridizations were unexpected, and the cause of them still remains to be determined. Plasmids pRH115 and pRH116 lacked b7, and the hybridization in the 3.0- to 3.5-kb region seen in these two cases may represent the Δ(33–43) hybrid fragment. The remaining hybridizations corresponded either to b2b sequences or to sequences present in the novel joints. All plasmids except pRH115 and pRH116 generated a band that comigrated with fragment b2b (Fig. 8). As shown in Fig. 7, f6 overlapped the clockwise end of b2b, so this hybridization is expected for plasmids that were not degraded in this region before circularization. Plasmids pRH115 and pRH116 generated bands of 7.4 kb that extensively hybridized to the probe, and they corresponded in size to one of the portions of b2b resulting from cleavage at the insertion, as described above. This confirms the identification of this fragment. The analysis with *Eco*RI indicated that sequences in fragment f3 are present in all plasmids, which indicates that the F DNA on these plasmids extends at least to 59.9F. The presence of the b2b sequences in the hybridization results shown in Fig. 8 indicates that these plasmids all contain, in addition, the F sequences extending from the clockwise end of f3 to the clockwise terminus of b2b at 61.7F.

The joint fragments produced during formation of these plasmids should contain some homology to b14 since the clockwise portion of b2b DNA is apparently present in all plasmids, and since no b1 DNA is present (which would have been detected by hybridization with f15 sequences in the probe). The joint fragments appear in characteristic positions for each class of Δtra F-prime plasmid. The joints for the Δtra F*proA*$^+$ plasmids have sizes of 1.4 ± 0.1 kb, the joints for the Δtra F*purE*$^+$ plasmids have sizes of 0.76 ± 0.01 kb, and the joints for the Δtra F*purE*$^+$ (*proC*$^+$) plasmids have sizes of 4.90, 6.42, and 8.60 kb for pRH130, pRH131, and pRH132, respectively. These results are consistent with those obtained by *Eco*RI. Representatives of the larger class of Δtra F *purE*$^+$ plasmids (pRH101 and pRH133; see Table 3) were not tested by hybridization. However, electrophoretic examination of the products of *Bgl*II digestion (data not shown) indicated that the joint fragment characteristic of the smaller class (e.g., pRH126) was absent from both pRH101 and pRH133. Instead, there was an additional fragment from both pRH101 and pRH133 DNA that comigrated with F fragment b12 (about 1.34 kb)

and that was not produced from either F or pRH126 DNA. This new 1.3-kb fragment is identified as the *Bgl*II-derived joint, an assignment consistent with the *Eco*RI data, which also indicated that the joints of pRH101 and pRH133 were 0.6 kb larger than the joints of the pRH126 class of plasmids. The simplest interpretation of the comigration of the joint fragments characteristic of each Δ*tra* F*purE*$^+$ plasmid class or of the Δ*tra* F*proA*$^+$ plasmids is that formation of these plasmids is a precise and repeatable event. The possibility that variable amounts of F DNA are present on these joint fragments, and that exactly compensating amounts of bacterial DNA are present such that the joint fragments comigrate, cannot be excluded, but seems unlikely. If this were true, the bacterial sites involved in formation of the Δ*tra* F*purE*$^+$ class of plasmids represented by pRH126, pRH127, pRH129, and pRH135 would still be clustered within a span of 0.5 kb—the amount of F DNA between *oriT* and the counterclockwise cleavage site defining *Bgl*II fragment b14. A similar conclusion may be reached for the *tra* F*proA*$^+$ plasmids pRH113 through pRH116.

The joint fragments for the Δ*tra* F*purE*$^+$ (*proC*$^+$) plasmids all had different sizes. In addition, pRH132 had a *Bgl*II fragment (7.7 kb) not present in plasmids pRH130 and pRH131. Using the maximum amount of F DNA (0.5 kb) that can be present on these fragments, we estimate from their sizes and the size of the additional *Bgl*II fragment present of pRH132 that the bacterial sites for circularization in the formation of pRH131 and pRH132 are 1.5 and 11.7 kb, respectively, counterclockwise to the site involved in formation of pRH130. These results agree well with results from digestion with *Eco*RI. Because b2b is present in these plasmids, the contribution to the variation in the sizes of the joints by differences in the amount of F present is limited to 0.5 kb.

The hybridization results thus confirm the previous conclusions that formation of Δ*tra* F*proA*$^+$ and Δ*tra* F*purE*$^+$ plasmids can be a precise event, and the data in Fig. 8 further indicate that the maximum variation in the amount of F DNA present in the vicinity of *oriT* is ±0.5 kb for the plasmid classes shown. We believe that it is likely that the variation is much less than this for the Δ*tra* F*proA*$^+$ and Δ*tra* F*purE*$^+$ plasmids shown.

DISCUSSION

The structures of the Δ*tra* F-prime plasmids reported here (Fig. 2) identify at least two (and possibly three) restricted regions on the bacterial chromosome at which specificity in the formation of this plasmid class occurs. The approximate location of these endpoints on the *E. coli* genetic map can be determined from the length of bacterial DNA carried by these plasmids, the physical location of the appropriate F integration sites, and the conversion factor of 41 kb per genetic minute (2). Since *lacI* is located near 7.9 min (2), and the clockwise terminus of $\alpha_3\beta_3$ is approximately 45.7 kb from a Mu insertion in *lacI* (21, 22), the clockwise terminus of $\alpha_3\beta_3$ should map near 6.8 min. Plasmids pRH113 through pRH116 contain approximately 142 kb of bacterial DNA immediately counterclockwise to $\alpha_3\beta_3$; therefore, their specific terminus is located near 3.3 min on the *E. coli* map, in the vicinity of *dapC* (2). $\alpha_4\beta_4$ is 239 kb from $\alpha_3\beta_3$ (15, 22), so its location on the genetic map should be near 12.6 min. Since the Δ*tra* F*purE*$^+$ plasmids contain approximately 38.6 kb of bacterial DNA located immediately counterclockwise to $\alpha_4\beta_4$, their specific terminus is located near *purE* at around 11.7 min. We note that this may be in the vicinity of the *fre-1* locus, a recombinational hot spot identified by Bresler et al. (4). The bacterial DNA carried by pRH130 and pRH131 may define an additional termination region at or near the IS*2* element between *lac* and *proC* at around 8.3 min. Specificity in these two cases is indicated by the close proximity (1.5 kb) of their bacterial termini in a region 150 kb removed from the selected marker. The endpoints near 3.2 and 11.7 min do not correspond in an obvious manner to previously mapped genetic elements in these locations (2).

The joint fragments of all six Δ*tra* F-prime plasmids that terminated near *dapC* appeared to be identical, even though they were derived from different Hfr strains with points of origin at either $\alpha_3\beta_3$ or at $\alpha_4\beta_4$. In contrast, the joint fragments of the Δ*tra* F-prime plasmids whose bacterial termini lie near *purE* differ by an average of 0.6 kb. This variation may indicate that there are two closely linked bacterial sites near *purE* that participate in Δ*tra* F-prime formation. The joint fragments of the Δ*tra* F-prime plasmids that terminate near *proC* differ by as much as 11.7 kb, which may be indicative of a kind of regional specificity (34). It is likely that the specific endpoints at each of these three sites are primarily determined by the bacterial nucleotide sequence. Since the degree of variation in bacterial termini differs at the three chromosomal regions, it seems unlikely that specific sequences of F (e.g., *oriT*) are solely responsible.

Specific bacterial endpoints were not observed by heteroduplex analysis of four Δ*tra* F*argG*$^+$ plasmids (17). This could indicate structural differences in the two different regions of the chro-

mosome, or it may have resulted from the more limited sample size in the previous study. Such structural differences in various regions of the *E. coli* chromosome are indicated by previous studies (25), which demonstrated that transconjugant yields in Hfr matings with *recA* recipients differ, depending on the integration site of F. Moreover, 22 of the 23 plasmids studied here had circularization events which occurred within the F *Eco*RI fragment f6 (pRH99 is the exception), whereas only two of the four Δ*tra* F*argG*$^+$ plasmids formed by circularization at a site predicted to lie within f6 (17).

The biological significance of this class of F-prime plasmid is uncertain. For example, these plasmids might be regarded as intermediates of the recombination process, recovered in this case because the recipients are *recA*, or they might represent aberrant entities that occur rarely in Hfr × F$^-$ matings. Moreover, many aspects concerning the molecular mechanisms of conjugal mating are still unclear (1, 11, 12). Various models for F-plasmid circularization include presence of cohesive ends (see, for example, references 12 and 29), recombination between directly repeated sequences on transferred segments of greater than unit length (27) (unlikely for plasmids formed in *recA* recipients [23]), and mediation of strand terminus rejoining by a membrane-protein complex (23). It may be that the processes that determine the endpoint specificity of these Δ*tra* F-prime plasmids occur before, and independent of, the actual circularization event.

We have considered two possible models to explain how certain chromosomal sequences become joined to the region near the *oriT* locus.

The first model suggests that the specificity is a consequence of F-specified circularization functions. These functions could take the form of a structure at *oriT* that recognizes not only the appropriate sequence of transferred F DNA in F$^+$ matings but also other bacterial sites (perhaps with a lower efficiency), in a manner formally analogous to recognition of secondary attachment sites by the *attP* region of λ (31). The endonuclease presumed to be active at *oriT* (35) might be involved in this process. Previously, Willetts (35) suggested that F-mediated chromosomal mobilization might occur without F integration as a result of initiation of transfer from a chromosomal sequence similar to *oriT*. Therefore, this first model would predict that the specific bacterial endpoints observed here may be related to sites where chromosomal mobilization occurs and that certain F mutants may be defective in this circularization process.

A second model to explain the endpoint specificity is that the circularization process occurs independently of specific recognition by F-specified functions. In other words, the circularization process would act upon whatever linear segments of DNA are presented to it. By this model, the similar plasmids would result from specific DNA segments whose lengths are determined before the circularization step. Since a single strand is transferred during conjugation (27), this could result from the presence of nicks, gaps, or nonstandard linkage in the transferred strand. Specific DNA segments could also result from specificity in degradation of random DNA lengths. One possible type of nonstandard linkage would be the covalent DNA-protein complexes identified in various organisms (see, for example, reference 10). Nicks or gaps might be produced in either the donor or recipient cell. Since many of the joint fragments appear to be identical in size, the single-strand termini of any nicks or gaps might be protected from exonucleases in some manner. The bacterial termini for pRH130 and pRH131 are located near the ends of a bacterial IS*2*. These plasmids might have been formed because of nicks generated in the vicinity of IS*2* as a result of recombinational functions associated with IS*2* (e.g., translocation or deletion). It may be that the other specific F-prime termini are determined by other unidentified translocatable elements. A prediction of the second model is that circularization-defective mutations would map in the bacterial DNA.

ACKNOWLEDGMENTS

We are grateful to H. Shizuya and M. Guyer for their constructive comments concerning these experiments. We also thank P. Broda and R. Curtiss III for providing their Hfr strains. The strain containing pRS27 was kindly provided by R. Skurray.

This research was supported by Public Health Service grant GM24589 from the National Institutes of Health.

LITERATURE CITED

1. **Achtman, M.** 1973. Genetics of the sex factor in Enterobacteriaceae. Curr. Top. Microbiol. Immunol. **60**:79–123.
2. **Bachmann, B., K. B. Low, and A. L. Taylor.** 1976. Recalibrated linkage map of *Escherichia coli* K-12. Bacteriol. Rev. **40**:116–167.
3. **Berg, C. M., and R. Curtiss III.** 1967. Transposition derivatives of an Hfr strain of *Escherichia coli* K-12. Genetics **56**:503–525.
4. **Bresler, S. E., S. V. Krivonogov, and V. A. Lanzov.** 1978. Scale of the genetic map and genetic control of recombination after conjugation in *Escherichia coli* K-12. Mol. Gen. Genet. **166**:337–346.
5. **Broda, P.** 1967. The formation of Hfr strains in *Escherichia coli* K12. Genet. Res. **9**:35–47.
6. **Broda, P., and P. Meacock.** 1971. Isolation and characterization of Hfr strains from a recombination-deficient strain of *Escherichia coli*. Mol. Gen. Genet. **113**:166–173.

7. **Childs, G. J., H. Ohtsubo, E. Ohtsubo, F. Sonnenberg, and M. Freundlich.** 1977. Restriction endonuclease mapping of the *Escherichia coli* K12 chromosome in the vicinity of the *ilv* genes. J. Mol. Biol. **117**:175–193.
8. **Clark, A. J., and A. D. Margulies.** 1965. Isolation and characterization of recombination deficient mutants of *Escherichia coli* K12. Proc. Natl. Acad. Sci. U.S.A. **53**: 451–459.
9. **Clowes, R. C., and W. Hayes.** 1968. Experiments in molecular genetics. John Wiley & Sons, Inc., New York.
10. **Coombs, D. H., and G. D. Pearson.** 1978. Filter-binding assay for covalent DNA-protein complexes: adenovirus DNA-terminal protein complex. Proc. Natl. Acad. Sci. U.S.A. **75**:5291–5295.
11. **Curtiss, R., III.** 1969. Bacterial conjugation. Annu. Rev. Microbiol. **23**:69–136.
12. **Curtiss, R., III, and R. G. Fenwick, Jr.** 1975. Mechanism of conjugal plasmid transfer, p. 156–165. *In* D. Schlessinger (ed.), Microbiology—1974. American Society for Microbiology, Washington, D.C.
13. **Curtiss, R., III, and D. R. Stallions.** 1969. Probability of F integration and frequency of stable Hfr donors in F^+ populations of *Escherichia coli* K-12. Genetics **63**: 27–38.
14. **Deonier, R. C., and R. G. Hadley.** 1980. IS2-IS2 and IS3-IS3 relative recombination frequencies in F integration. Plasmid **3**:48–64.
15. **Deonier, R. C., G. R. Oh, and M. Hu.** 1977. Further mapping of IS2 and IS3 in the *lac-purE* region of the *Escherichia coli* K-12 genome: structure of the F-prime ORF203. J. Bacteriol. **129**:1129–1140.
16. **De Witt, S. K., and E. A. Adelberg.** 1962. The occurrence of a genetic transposition in a strain of *Escherichia coli*. Genetics **47**:577–585.
17. **Guyer, M. S., N. Davidson, and A. J. Clark.** 1977. Heteroduplex analysis of *traΔ* F′ plasmids and the mechanism of their formation. J. Bacteriol. **131**:970–980.
18. **Hadley, R. G., and R. C. Deonier.** 1979. Specificity in the formation of type II F′ plasmids. J. Bacteriol. **139**: 961–976.
19. **Hotchkiss, R. D.** 1974. Models of genetic recombination. Annu. Rev. Microbiol. **28**:445–468.
20. **Howard-Flanders, P., and L. Theriot.** 1966. Mutants of *Escherichia coli* K-12 defective in DNA repair and in genetic recombination. Genetics **53**:1137–1148.
21. **Hsu, M.-T., and N. Davidson.** 1972. Structure of inserted bacteriophage Mu-1 DNA and physical mapping of bacterial genes by Mu-1 DNA insertion. Proc. Natl. Acad. Sci. U.S.A. **69**:2827–2837.
22. **Hu, S., E. Ohtsubo, and N. Davidson.** 1975. Electron microscope heteroduplex studies of sequence relations among plasmids of *Escherichia coli:* structure of F13 and related plasmids. J. Bacteriol. **122**:749–763.
23. **Kingsman, A., and N. Willetts.** 1978. The requirements for conjugal DNA synthesis in the donor strain during F*lac* transfer. J. Mol. Biol. **122**:287–300.
24. **Lennox, E. S.** 1955. Transduction of linked genetic characters of the host by bacteriophage P1. Virology. **1**:190–206.
25. **Low, B.** 1968. Formation of merodiploids in matings with a class of *rec*$^-$ recipient strains of *Escherichia coli* K12. Proc. Natl. Acad. Sci. U.S.A. **60**:160–167.
26. **Low, K. B.** 1972. *Escherichia coli* K-12 F-prime factors, old and new. Bacteriol. Rev. **36**:587–607.
27. **Ohki, M., and J.-I. Tomizawa.** 1968. Asymmetric transfer of DNA strands in bacterial conjugation. Cold Spring Harbor Symp. Quant. Biol. **33**:651–657.
28. **Ohtsubo, E., and M.-T. Hsu.** 1978. Electron microscope heteroduplex studies of sequence relations among plasmids of *Escherichia coli:* structure of F100, F152, and F8 and mapping of the *Escherichia coli* chromosomal region *fep-supE-gal-attλ-uvrB*. J. Bacteriol. **134**:778–794.
29. **Pardee, A. B., F. Jacob, and F. Monod.** 1959. The genetic control and cytoplasmic expression of "inducibility" in the synthesis of β-galactosidase by *E. coli*. J. Mol. Biol. **1**:165–178.
30. **Sharp, P. A., M.-T. Hsu, E. Ohtsubo, and N. Davidson.** 1972. Electron microscope heteroduplex relations among plasmids of *E. coli*. I. Structure of F-prime factors. J. Mol. Biol. **71**:471–497.
31. **Shimada, K., R. A. Weisberg, and M. E. Gottesman.** 1972. Prophage lambda at unusual chromosomal locations. I. Location of the secondary attachment sites and the properties of the lysogens. J. Mol. Biol. **63**:483–503.
32. **Skurray, R. A., H. Nagaishi, and A. J. Clark.** 1978. Construction and *Bam*HI analysis of chimeric plasmids containing *Eco*RI DNA fragments of the F sex factor. Plasmid **1**:174–186.
33. **Thompson, R., and M. Achtmann.** 1978. The control region of the F sex factor DNA transfer cistrons: restriction mapping and DNA cloning. Mol. Gen. Genet. **165**: 295–304.
34. **Weinstock, G. M., and D. Botstein.** 1979. Regional specificity of illegitimate recombination associated with the translocatable ampicillin-resistance element Tn*1*. Cold Spring Harbor Symp. Quant. Biol. **43**:1209–1215.
35. **Willetts, N.** 1972. The genetics of transmissable plasmids. Annu. Rev. Genet. **6**:257–268.